Low-field magnetic study on the $Li_xNi_{1-x}O$ system

A. Bajpai and A. Banerjee
Inter University Consortium for DAE Facilities, University Campus, Khandwa Road, Indore 452001, India
(Received 19 September 1996)

A series of polycrystalline $Li_xNi_{1-x}O$ is prepared by a solid-state route for x ranging from 0.1 to 0.5. The Rietveld profile refinement of x-ray powder-diffraction data shows that the samples with $x \geqslant 0.3$ apparently possess two types of atomic arrangement in the cationic plane in a direction perpendicular to the cubic $\langle 111 \rangle$ direction of the parent cubic lattice of NiO. Low-field linear and nonlinear ac susceptibility and dc magnetization measurements show the importance of the ordering of cations in the magnetic properties. The history dependence of dc magnetization, field and frequency dependence of linear and nonlinear ac susceptibility as well as the divergence of nonlinear ac susceptibility allow us to infer a spin-glass-like phase in the samples with $x = 0.3$ and 0.35. [S0163-1829(97)03718-1]

I. INTRODUCTION

The $Li_xNi_{1-x}O$ system retains the cubic rocksalt structure of the parent compound, NiO up to a critical composition, beyond which it shows a transition to hexagonal symmetry. The structural properties are well described in the literature.[1–6] The magnetic structure is interpreted in a variety of ways, ranging from ferrimagnetic,[1,7] ferromagnetic,[8] enhanced antiferromagnetism,[9] superparamagnet,[5] and spin glass.[4] Interestingly, most magnetic and transport property results are not compatible with spectroscopy results[9,10] and this is another subject matter of controversy.

The common assumption regarding the interpretation of magnetic and transport properties is that the Li substitution in NiO changes the charge state of the cation from Ni^{2+} to Ni^{3+}. The hole, thus created, can conduct and the system shows semiconducting behavior with a band gap, $E_g \approx 0.2$ eV (Ref. 11) (the parent compound NiO, when pure and stoichiometric, is an antiferromagnetic (AFM) insulator with a band gap of the order of 5 eV). The magnetic study on Li-doped NiO was initiated by Goodenough, Wickham, and Croft.[1] Their dc magnetization measurement has shown that the system $Li_xNi_{1-x}O$ remains antiferromagnetic for $x \leqslant 0.3$. A ferrimagnetic phase along with a rhombohedral distortion of the lattice was observed for $x \geqslant 0.3$. They assumed the partial ordering of Li and Ni ions in an alternate set of planes which couple antiparallel to one another. Later, the system $LiNiO_2$ was considered to be a potential candidate for a spin-half two-dimensional (2D) trigonal lattice antiferromagnet resulting in a quantum liquid ground state.[12] There are reports supporting this suggestion.[7] Contrary to this, the system was shown to behave as a weakly coupled 2D Ising ferromagnet via 90° Ni-O-Ni coupling in $LiNiO_2$.[8] In some cases, 90° indirect exchange coupling giving rise to ferromagnetic clustering, resulted in a superparamagnetic phase as concluded from dc magnetic susceptibility and ESR measurements.[5] Spin-glass behavior was also observed in some of the samples with $x = 0.5$ composition, at relatively lower temperatures (≈ 9 K). X-ray and neutron diffraction with Rietveld refinement analysis has shown that there are always some Ni atoms occupying sites in the Li layers and this profoundly affects the magnetic behavior.[4] Further, it was shown that the degree of cation ordering is sensitive to the annealing rate during sample preparation.[2,3] A systematic study made recently on Li-Ni-O in a wide composition range shows that two different solid solutions are present in the system.[6] One is the substituted solid solution with formula unit $Li_xNi_{1-x}O$, where both Li and Ni are randomly distributed in the cationic sites. Second is the ordered solid solution, $Li_{2x}Ni_{2-2x}O_2$, having preferred occupation of the two cations in alternate planes. This is usually referred to as $LiNiO_2$. However, stoichiometric $LiNiO_2$ is very difficult to prepare and there is a small Li deficiency, due to Ni atoms occupying Li sites.[4,6]

Spectroscopy results, on the other hand, suggest that the hole lies primarily on oxygen $2p$ rather than the Ni $3d$ band.[9,10] It was shown using oxygen $K\alpha$ edge absorption spectroscopy that the extra holes introduced by Li doping have about 70% O $2p$ character.[9]

The aim of the present study is to understand the nature of the disordered magnetic phases in the system Li-Ni-O and its correlation to cationic order considering all types of cationic interactions proposed earlier on a similar system. We have prepared samples with a wide composition range, adopting similar heat-treatment procedure, to find out the systematic in the cationic arrangement with composition and to identify the particular arrangement responsible for the resulting magnetic properties. For the magnetic study we have concentrated on the samples with $x = 0.3$ and $x = 0.35$ composition. We have found that these two samples show frequency (f) and field (h) dependent sharp peaks in linear and nonlinear ac susceptibility (ac-χ) at around 200 K. This is similar to other metastable magnetic systems with macroscopic time scales.[13,14] Around this temperature range earlier studies have shown a ferrimagnetic[1,7] or superparamagnetic phase,[5] for a similar composition. To our knowledge one of the most important measurements of low field, linear, and nonlinear ac-χ measurements has not been done in the above-mentioned system which has given enough of an indication, both theoretically and experimentally[4] to show a variety of magnetic order including the spin-glass phase. We have chosen the low-field ac and dc techniques so that if there is a spin-glass-like phase, it does not become smeared by the application of high magnetic fields. We have tried to concen-

trate on the nonlinear ac-χ since the theory[15] and experiments[16,17] in the spin-glass systems have shown a critical behavior in nonlinear ac-χ rather than linear ac-χ. Our observations give evidence for a spin-glass-like phase in the system and we try to justify our results on the basis of possible exchange interactions.

II. SAMPLE PREPARATION AND CHARACTERIZATION

Samples are prepared by the solid-state route using stoichiometric mixtures of NiO black and Li_2CO_3. We have realized that it is easier to form the compound using NiO black as the starting material. Using NiO green as the starting material, however, requires prolonged heat treatments (HT), especially on the higher doping side, to form the desired composition. Prolonged HT often result in uncontrolled Li deficiency in the samples.[4] The mixture is intimately grounded and pelletized under a pressure $\approx 10^9$ Pa. Heat treatments are given in pellet form, in the temperature range varying from 700 (for $x \leqslant 0.35$) to 900 °C (for $x \geqslant 0.4$). Samples with $x < 0.35$ are heated for periods up to 24 h in alumina boats. Samples with $x > 0.35$ are given intermediate grindings between HT extending up to 48 h. At the end of HT the samples are allowed to cool slowly to room temperature.

X-ray-diffraction (XRD) measurements are made using Rigaku Rotoflex RTC 300 RC powder diffractometer with Cu $K\alpha$ radiation. The patterns are collected in the angular range of 10°–90° at the interval of 0.01°. X-ray data for $x = 0.1$, 0.2, 0.3, 0.35, 0.4, and 0.5 samples are analyzed by Rietveld profile refinement method using the modified version of the profile refinement program by Young *et al.*[18] The program acquires a least-squares fit between observed and calculated intensities by adjusting the physical parameters like cell constants, temperature factor, atomic coordinates, composition as well as instrumental parameters. Peak profile function for fitting is chosen as a pseudo-Voigt function. We have obtained the best fit for our samples considering the following structural patterns:

(1) Samples with $x < 0.3$ are fitted to a cubic rocksalt structure (space group $Fm3m$) with cationic site (0,0,0) (for Li and Ni) and anionic site (0,0, 1/2). This phase corresponds to the formula unit $Li_xNi_{1-x}O$.

(2) Samples with $x \geqslant 0.3$ are fitted to hexagonal symmetry ($R3m$). The best fit is obtained by considering two cationic arrangements for all the samples with $x \geqslant 0.3$. This apparently results in the following two phases in the same structure.

Phase A: In this phase, both Li and Ni share the same cationic site (0,0,0) and the anionic (oxygen) site is (0,0,1/2). This will be referred to as the random phase (as Li replaces Ni randomly). This corresponds to formula unit $Li_xNi_{1-x}O$.

Phase B: Here the first cationic site is (0,0,0) for Ni, second cationic site (0,0,1/2) for Li or Ni, and anionic site $(0,0,z)$ with $z = 1/4$. This will be referred to as the ordered phase, usually quoted as $LiNiO_2$ with doubled c axis.[6] This corresponds to the formula unit $Li_{2x}Ni_{2-2x}O_2$. This phase is in accordance with the perfect ordering of Li and Ni in an alternate set of planes as is described in the literature. Even in this ordered phase there can be some Ni atoms occupying Li sites.[4]

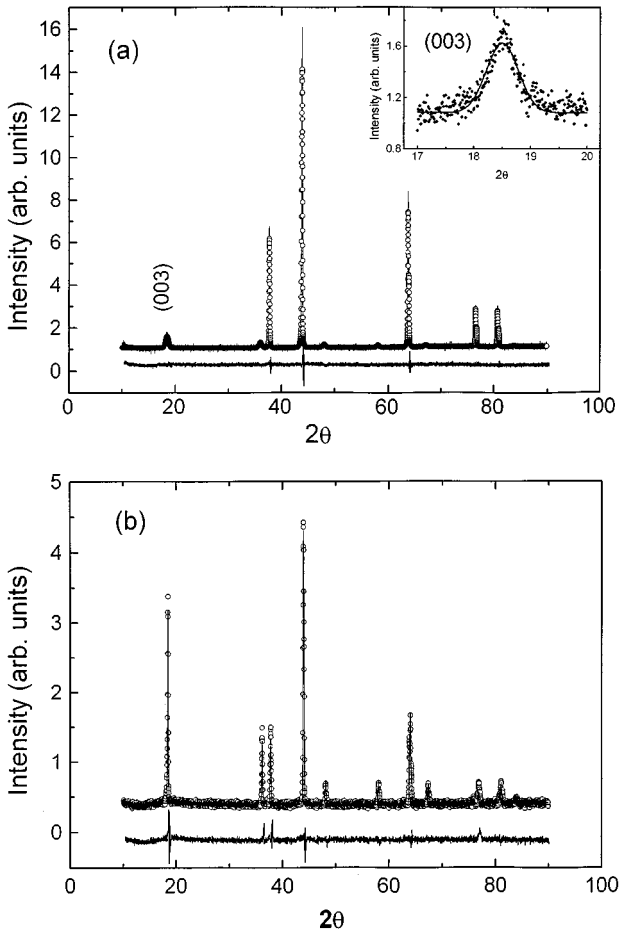

FIG. 1. (a) The observed (open circles), fitted (solid line) and the difference (lower curve) XRD patterns for the sample with $x = 0.35$. Inset shows the observed (closed circles) and fitted (solid line) (003) peak. (b) The observed (open circles) and fitted (solid line) XRD patterns along with their difference curve for the sample with $x = 0.5$.

Our Rietveld analysis shows that this indeed is the case for some of our samples. Figure 1(a) shows the observed and fitted intensities along with their difference curve for the sample with $x = 0.35$. The occurrence of the ordered phase is indicated by the presence of (003) and certain other superlattice reflections. The inset of Fig. 1(a) shows the observed and the fitted intensity of (003) peak. In Fig. 1(b) we have plotted the observed and calculated patterns for a sample with $x = 0.5$. Here we can see that the relative intensity of (003) superlattice reflection increases as the percentage of ordered phase increases in the sample with $x = 0.5$, as compared to that of the sample with $x = 0.35$. The fraction of the ordered phase in the $x = 0.5$ sample, though large, is still about 82% as listed in Table I. Since the sample with $x = 0.5$ has the largest fraction of ordered phase, all the reflections pertaining to ordered phase are clearly seen in Fig. 1(b).

Composition $x = 0.3$ is around the critical composition[2] for which hexagonal splitting of the peaks as well as appearance of peaks like the (003) peak are observed in the XRD data. Since samples with the $x = 0.3$ composition are around the critical concentration, it is possible to make two samples by slightly different preparation conditions, in such a way

TABLE I. Refined parameters and various agreement factors as obtained from Rietveld analysis. a_c, v_c, and a_h, v_h refer to lattice parameters (in Å) and cell volume for cubic and hexagonal unit cell, respectively. The % indicates the calculated mass percentage of the ordered or the random phase. Agreement factors, R_p (R pattern), R_w (R-weighted pattern), and R_{ex} (R expected) are defined in Ref. 18.

	Cubic fitting Random phase		Hex fitting										
			Random phase				Ordered phase						
x	a_c	v_c	a_h	c_h	v_h	%	a_h	c_h	v_h	%	R_p	R_w	R_{ex}
0.1	4.1622(1)	72.11(3)									4.88	6.21	2.82
0.2	4.1594(2)	71.96(1)									4.71	5.92	2.79
0.3*			2.9155(3)	7.1513(7)	52.72(3)	100					5.95	7.70	3.58
0.3			2.9107(2)	7.1411(7)	52.40(3)	81.83	2.9023(7)	14.2263(1)	103.77(5)	18.17	6.14	7.70	3.89
0.35			2.9096(1)	7.1263(3)	52.25(1)	63.23	2.9092(2)	14.2442(3)	104.4(1)	36.74	4.74	6.08	2.88
0.4			2.9077(3)	7.1221(1)	52.15(2)	27.52	2.8913(3)	14.2355(4)	103.06(8)	72.48	4.43	5.67	4.73
0.5			2.9027(2)	7.0826(1)	51.68(1)	18.08	2.8936(2)	14.2428(5)	103.28(4)	81.92	4.80	6.41	4.77

that in one batch, the ordered phase does not develop. This is indicated by the absence of the peak owing to the (003) reflection as well as the splitting in the peaks at higher angles corresponding to the ordered phase. However, the sample shows the splitting due to the rhombohedral distortion in the random phase. This sample is indicated by 0.3* and the refined parameters are given in Table I. The other $x=0.3$ sample (indicated by 0.3 in Table I) shows a small (003) reflection and splitting at higher angles corresponding to an ordered phase of about 18%.

Table I shows that in the random phase lattice parameters and cell volume show a systematic decrease with an increase in Li concentration, as expected. However, the refined lattice parameters of the ordered phases are slightly less than the random phase for any composition because of the preferential ordering of the cations. The lack of a systematic in the ordered phase indicates that this phase is Li deficient and some of the Li sites are occupied by Ni.

III. EXPERIMENTAL DETAILS

A. ac susceptibility measurements

Low-field ac-χ measurements are made using a homemade ac-susceptibility bridge. The reference sine wave of a Stanford Research System lock-in amplifier (LIA), model SR 850, drives the primary coil and the response of an oppositely wound pair of secondaries is picked up by the same LIA. Real and imaginary parts of the induced voltage as well as its higher harmonics, if induced magnetization is nonlinear, can be simultaneously picked up by this LIA. The sample and a platinum resistance thermometer are attached to a sapphire rod that goes inside a double walled glass cryostat. The coil system remains in the LN_2 bath whereas the temperature is regulated inside an evacuated glass cryostat. Temperature is controlled with an accuracy of 50 mK, using a homemade temperature controller and with an accuracy of 10 mK using a LakeShore temperature controller model DRC-93CA. The bridge is fully automated and calibrated using high-purity paramagnetic salts; Er_2O_3 and Gd_2O_3. The estimated sensitivity of this system is of the order of $\approx 10^{-7}$ emu. The magnitude and the phase of the applied magnetic field is derived from the primary current by measuring the voltage across a standard resistor connected in series with the primary coil. Samples are in the form of rectangular pellets of approximately $7\times3\times2$ mm^3 dimension.

B. dc magnetization measurements

Low-field dc magnetization measurements are made using an indigenously developed vibrating sample magnetometer. The arrangement is similar to that described by Foner.[19] Here a loudspeaker is used as the vibrating system and a lock-in amplifier as the detection system (Stanford Research Systems model SR LIA 530). The sample is vibrated in a uniform dc field produced by a copper solenoid and induced voltage is detected by a pair of pickup coils. The cryostat and temperature measurement system is similar to that described for an ac-χ setup. This setup is also calibrated with Er_2O_3 and Gd_2O_3. Sensitivity of the setup is better than 10^{-4} emu in the measured field range.

IV. RESULTS AND DISCUSSION

In ac-susceptibility measurements, the magnetization m can be expanded[20] with respect to an applied magnetic field h as

$$m=m_0+\chi_1 h+\chi_2 h^2+\chi_3 h^3+\cdots, \tag{1}$$

where χ_1 is the linear susceptibility and $\chi_2,\chi_3\ldots$ are the nonlinear susceptibilities. The magnetization m has an inversion symmetry with respect to the sign of h thus $\chi_2=\chi_4=\cdots 0$ in the absence of any superimposed dc magnetic field. Here it should be noted that when there is a spontaneous magnetization or internal field in the system, one may observe χ_2, χ_4, etc. due to the breaking of the inversion symmetry even by the earth's magnetic field.

Figure 2 shows the temperature variation of the real $\chi_1(r)$ and imaginary $\chi_1(i)$ parts of the first harmonic ac-χ for the $x=0.3$ sample. We observe a sharp peak in both $\chi_1(r)$ and $\chi_1(i)$ around 210 K having a peak width of about 2% of the temperature of the peak (T_c), and a broad hump-like structure at the lower temperature region is observed in $\chi_1(r)$ but $\chi_1(i)$ practically remains zero for this temperature range. Similar behavior is also observed in $\chi_1(r)$ and $\chi_1(i)$

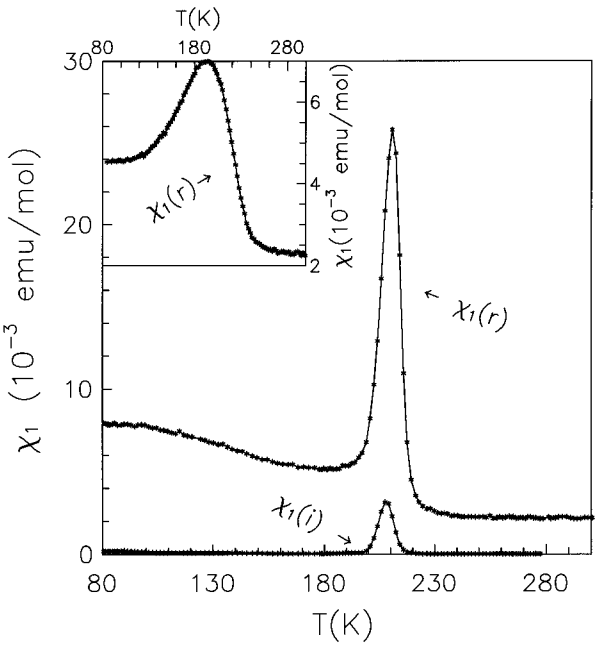

FIG. 2. $\chi_1(r)$ (circles) and $\chi_1(i)$ (triangles) plotted against temperature for the sample with $x=0.3$. Inset shows the $\chi_1(r)$ plotted against temperature for $x=0.3$* sample in which ordered phase did not develop (as indicated by 0.3* in Table I).

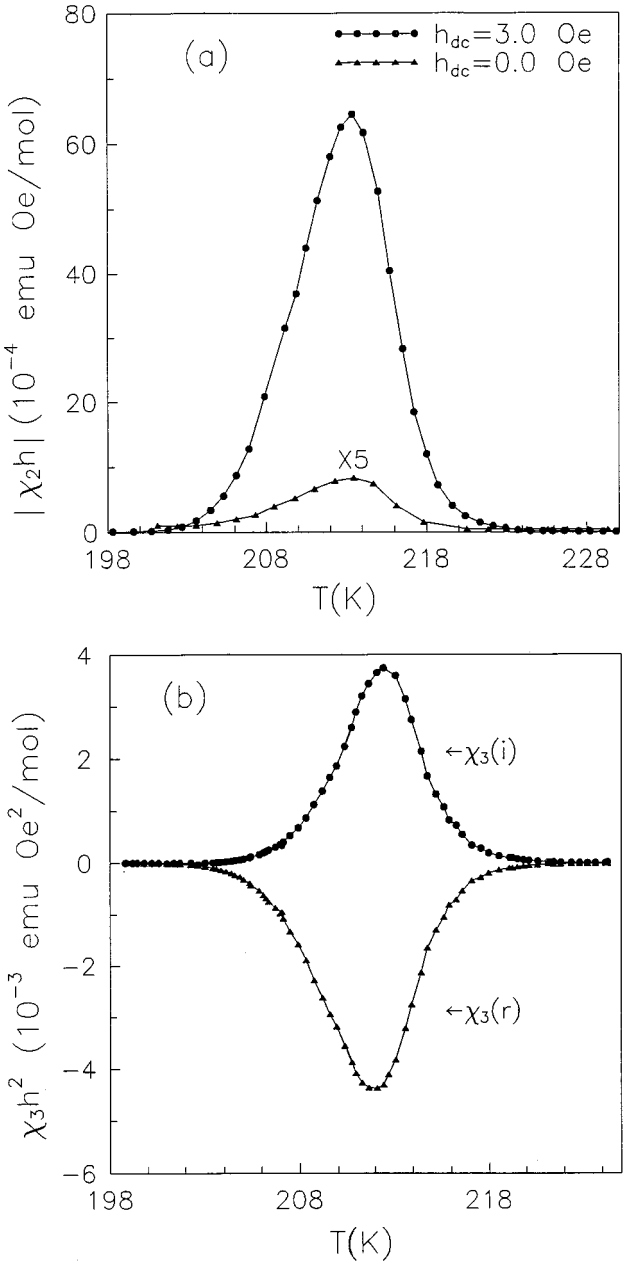

FIG. 3. (a) $|\chi_2 h|$ plotted against temperature in a superimposed dc field and in zero (applied) dc field (5 times $\chi_2 h$) for the sample with $x=0.3$. (b) $\chi_3(r)$ (triangles) and $\chi_3(i)$ (circles), plotted against temperature, for the sample with $x=0.3$.

for the sample with $x=0.35$. Earlier studies have predicted a ferrimagnetic[1,7] and a superparamagneticlike[5] transition for a similar composition around the temperature range where we have observed the sharp peaks in both $\chi_1(r)$ and $\chi_1(i)$. First we consider the broad humplike structure in $\chi_1(r)$ observed below the sharp peak in the lower temperature region. The $\chi_1(i)$ practically remains zero in this temperature range indicating that there is no magnetic loss or there is no opening of the M-H loop. Although, strong nonlinearity develops just around the transition as indicated by the presence of second and third harmonics of ac-χ in Figs. 3(a) and 3(b). There is no signature of spontaneous magnetization (as indicated by the absence of χ_2) below the sharp peak, neither in the earth's magnetic field nor in the superimposed dc field. There is no detectable signature of nonlinearity (absence of χ_3) in this temperature range. Similar behavior is also observed in the samples with $x=0.35$. These observations rule out the possibility of the low-temperature phase being a ferrimagnetic one.

As we have seen from the structural analysis, both the samples with $x=0.3$ and 0.35 possess a random phase as well as an ordered phase. Since there are no detectable harmonics and very a small opening of the M-H loop, the low-temperature phase may be the antiferromagnetic response of the random phase. To check this point we measured ac-χ on the $x=0.3$ sample where the ordered phase could not develop (shown as 0.3* in Table I). Indeed, we do not find any sharp peak as is observed in the other 0.3 sample (Fig. 2), having 18% of the ordered phase. In the 0.3* sample $\chi_1(r)$ is quite broad resembling a polycrystalline antiferromagnet as shown in the inset of Fig. 2. One can note that the peak width is about 150 K and though the paramagnetic tail of this and the other 0.3 sample coincide, the maximum change in the susceptibility is quite small as compared to the other 0.3 sample. Here we mention that we reprepared all the compositions from $x=0.1$ to $x=0.5$, following the same preparation method. We could reproduce all the results. Though there was a variation of a few Kelvin in magnetic T_c in some of the samples, that can be attributed to a slight difference in the ratio of ordered to random phase in the samples.

The sharp rise and fall of ac-χ, is observed in the $x=0.3$ sample where the ordered phase starts building up (Table I). To ascertain the magnetic phase we have measured the ac-χ over a wide range of frequencies for a fixed ac field and a wide range of fields for a fixed frequency for the samples with $x=0.3$ and 0.35. We find that the field or frequency variations affect both the magnitude and temperature of the susceptibility peak but do not have any significant

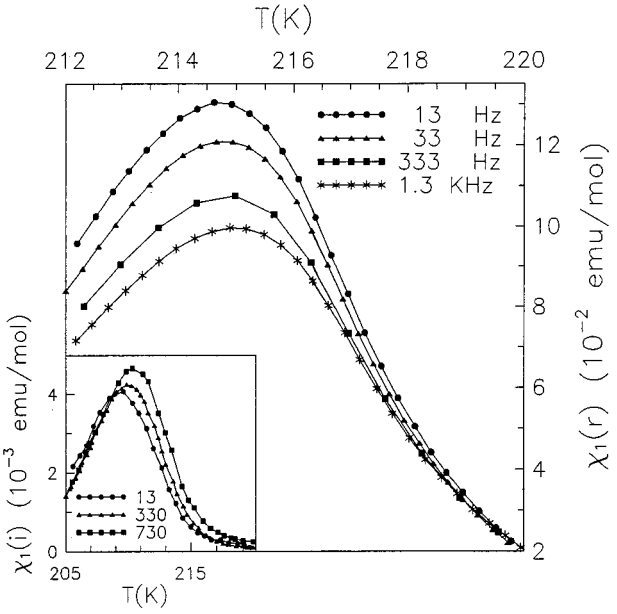

FIG. 4. Frequency dependence of $\chi_1(r)$ for the sample with $x=0.35$. Inset shows the frequency dependence of $\chi_1(i)$ for the sample with $x=0.3$ measured at 13, 330, and 730 Hz.

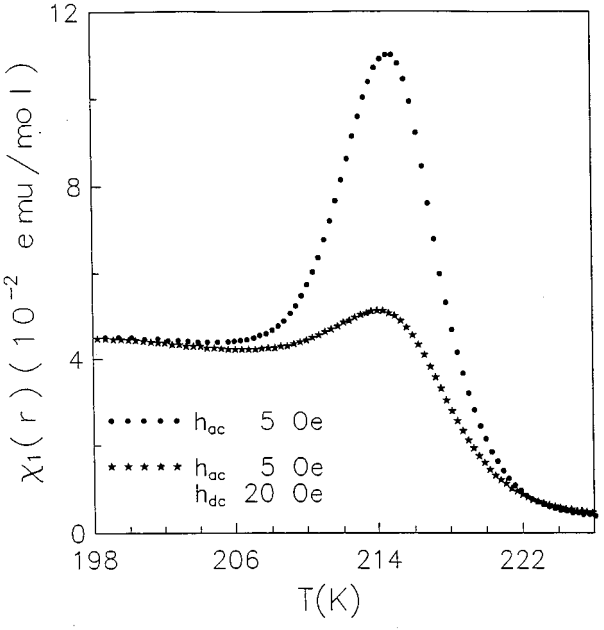

FIG. 6. $\chi_1(r)$ in a superimposed dc field and zero dc field for the sample with $x=0.35$.

effect on it above the transition region. Figure 4 shows the frequency dependence of $\chi_1(r)$, around the transition for the sample with $x=0.35$. The inset of Fig. 4 shows the frequency dependence of $\chi_1(i)$ for the other sample ($x=0.3$). We observe that the peaks in $\chi_1(r)$ shift to high temperature and decrease in magnitude with the increase in the frequency. On the other hand, the peaks in $\chi_1(i)$ increase in magnitude but shift to high temperature with the increase in frequency. Figure 5 shows the shift in the peak of the $\chi_1(r)$ with the measuring ac field. The inset of Fig. 5 shows

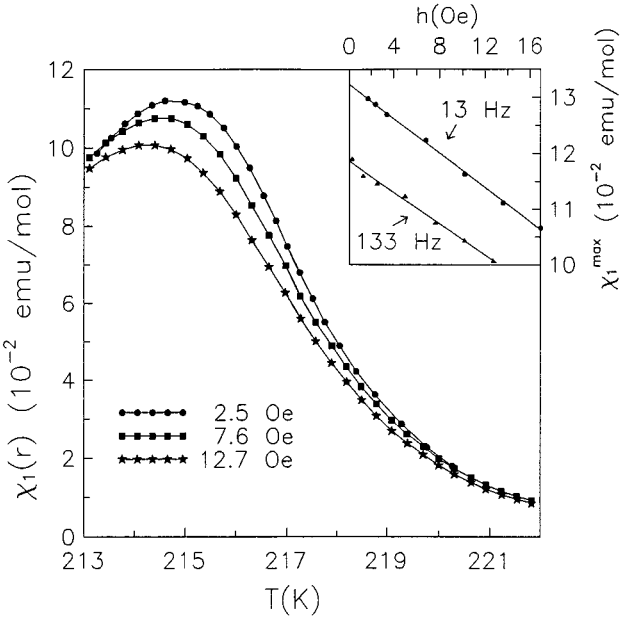

FIG. 5. Field dependence of $\chi_1(r)$, plotted against temperature for the sample with $x=0.35$. Inset shows χ_1^{max} vs field at 13 and 133 Hz for the sample with $x=0.35$.

the change in the peak value of the real part of $\chi_1(r)$ ($|\chi_1^{max}(r)|$) with the field. These features are typical signatures of systems with macroscopic relaxation times like spin glasses or superparamagnets.[13,14] A superparamagnetic system is expected to show a shift in χ_1 over a wide temperature range, much above the blocking temperature, with the change in field and frequency.[14] Whereas in a spin glass, all the curves merge above the transition[13,14] as depicted in Figs. 4 and 5. We have seen that in our case, the sharp features in ac-χ are suppressed by the application of a small superimposed dc field of the order of 20 Oe, but does not have any noticeable effect at as high temperatures as shown in Fig. 6. It should be noted that a superimposed dc field is expected to suppress the ac-χ over a wide temperature range above the blocking temperature for a superparamagnet[14] or a cluster glass.[21] On the contrary a spin glass does not show any such effect.[14]

A superparamagnet shows a broad negative χ_3 spanning over the whole temperature range much beyond the blocking temperature,[14,17] as compared to a spin glass that shows a sharp negative χ_3 only around the transition, similar to what is observed in Fig. 3(b). Theoretically,[15] the linear susceptibility of a spin-glass shows a cusp whereas the nonlinear susceptibilities are expected to diverge in the limit of $h\rightarrow 0$, and $f\rightarrow 0$. Though it is difficult to measure the divergence experimentally, the criticality of χ_3 is already found in some spin glasses.[13,16] We have plotted the magnitude of the peak value of χ_3 ($|\chi_3^{max}|$) as a function of applied field and frequency in Figs. 7(a) and 7(b). From Figs. 7(a) and 7(b) one can conclude that the nonlinear susceptibility will diverge in the limit of $h\rightarrow 0$ and $f\rightarrow 0$. One can find out from the inset of Fig. 5 that the linear term also shows a rise but it is much slower than that of the nonlinear term. We would like to mention that χ_5 also shows similar behavior for our samples. Higher harmonics would not show a divergence for a ferromagnetic or ferrimagnetic system in these limits. On

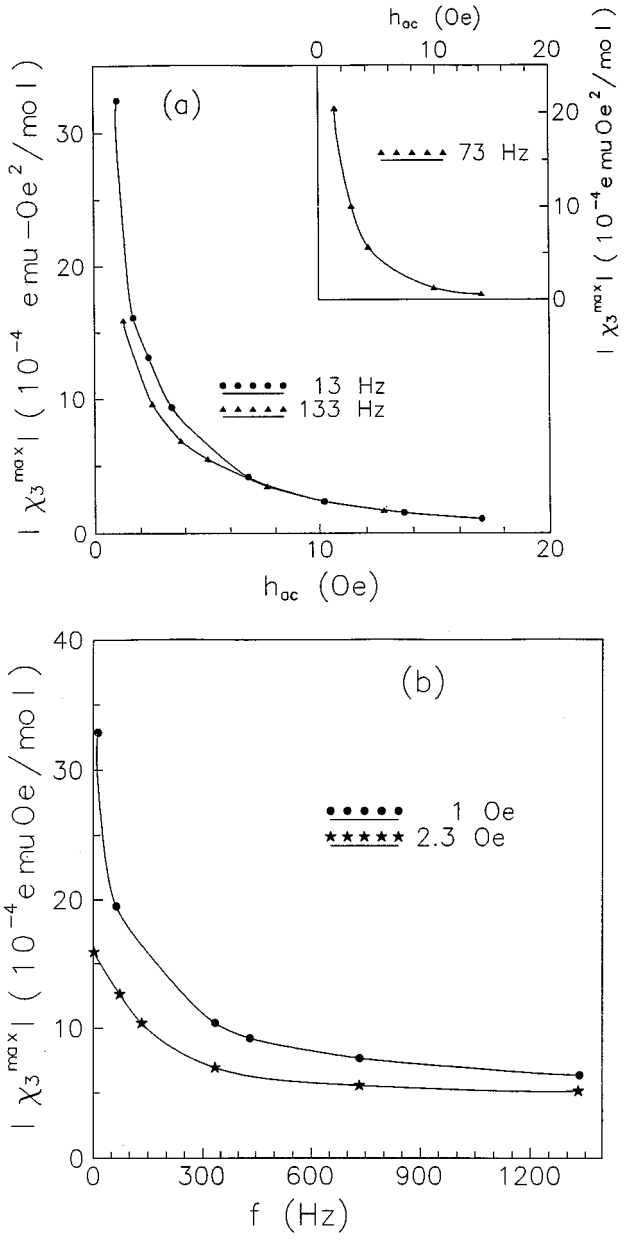

FIG. 7. (a) $|\chi_3^{max}|$ vs applied ac field for the sample with $x=0.35$ measured at 13 and 133 Hz. Inset shows the same for the sample with $x=0.3$ at 73 Hz. (b) $|\chi_3^{max}|$ vs frequency for the sample with $x=0.35$ measured in 1 and 2.3 Oe.

the contrary, a ferro or ferrimagnetic system will approach linearity with decreasing field. Even anisotropy-driven systems or domain-wall dynamics[22] are not expected to show such a response of nonlinear susceptibility, apart from having other major differences than our observations.

Figure 8 shows the field-cooled (FC) and zero-field-cooled (ZFC) dc magnetization curves for the $x=0.35$ sample. There is a bifurcation of FC and ZFC curves, as expected in spin-glass-like systems. We observe that the dc susceptibility (dc-χ) for all the fields overlap above the transition. Unlike our results a significant field dependence in dc-χ is found in superparamagnets[14] and in cluster glasses[21] much above the transition temperature. The FC curves in Fig. 8 show an uplift and similar behavior is also observed for the $x=0.5$ samples, at much lower temperatures, by

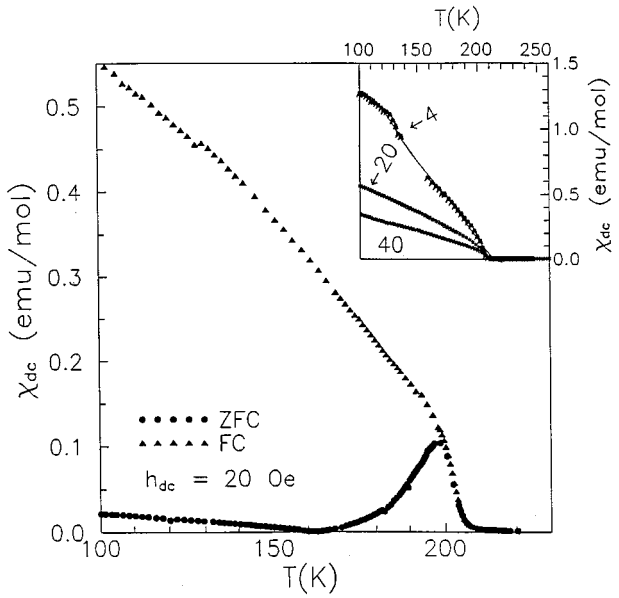

FIG. 8. Field-cooled (FC) and zero-field-cooled (ZFC) dc-χ plotted against temperature for the sample with $x=0.35$. Inset shows the FC dc-χ, measured at 4, 20, and 40 Oe.

Reimers, Li, and Dahn.[4] They have prepared the $x=0.5$ sample by different techniques. Samples are formed in the ordered phase ($LiNiO_2$) where some Ni atoms essentially occupy Li layers. They have found that the rise in FC dc-χ increases with the increase in the percentage of Ni occupying the Li layer and the steepest rise is found in a sample where maximum percentage of Ni (more than 10%) occupy Li layers. In our case with 30 and 35 % of Li doping, interlayer Ni-O-Ni interaction is expected to be large which is probably responsible for the removal of the degeneracy in the FC state.

Now we discuss the various magnetic interactions in the Li-Ni-O system.

(a) 180° Ni^{2+}-O-Ni^{2+} interaction which is an antiferromagnetic superexchange interaction, as in pure NiO.

(b) 180° Ni^{3+}-O-Ni^{3+} interaction, again antiferromagnetic. Here one assumes that Ni^{2+} has gone to a Ni^{3+} charge state due to Li doping although the amount of Ni^{3+} may not be equivalent to the dopant as some of the holes can remain with oxygen itself, as suggested by spectroscopy experiments.

(c) Ni^{2+}-O-Ni^{3+} interaction can be both AFM and FM. The nature and sign of this interaction depend upon the degree of distortion in the system,[1] as well as the low- or high-spin state of Ni^{3+}. However, it is a matter of controversy whether the crystalline field is large enough to break Hund's third rule[9,23] since a larger crystalline field makes the low-spin state of Ni^{3+} more probable.[1] This interaction may depend on the distance between cations which can be randomly varying depending on Li site.

(d) In the ordered phase with alternate layers of Li and Ni, the nearest-neighbor low spin Ni^{3+}, can couple through 90° Ni-O-Ni interaction resulting in ferromagnetic ordering within the plane.[24] It is worth mentioning here that even in the perfectly ordered phase there can be some Ni atoms occupying Li sites and there can be much stronger 180° interlayer coupling.

(e) Considering Ni^{3+} to be in the low-spin state, the diamagnetic Li^+ ions group with low spin Ni^{3+} to form polarons, and if Ni^{3+} polarons induce local Jahn-Teller distortions, the crystalline field of the neighboring Ni^{2+} ions will also be affected. This can induce a high-spin Ni^{2+} (d^8), ion to go into a low-spin ($S=0$) state by splitting of the e_g doublet.[25] The magnetic coupling of such an ion with its neighbor can be spin independent or unpredictable.

(f) High-spin Ni^{2+}-O-Ni^{2+} interaction when the ''hole'' lies with oxygen. This can also be ferromagnetic.

(g) The direct Ni-Ni exchange interaction is supposed to be very small in this system.

Since this system can have disorder as well as magnetic interactions varying in sign and strength, there can be a possible competition in exchange coupling. Since the spin-glass-like features appear in $x=0.3$ and $x=0.35$ samples in which an ordered phase has formed, we focus on the ordered structure where Li goes on preferential sites. Here, there would be a Ni+Li layer in between two Ni layers (only the stoichiometric $x=0.5$ sample will have alternate layers of Ni and Li). If the Li atom replaces Ni, making some of the adjacent Ni^{2+} become Ni^{3+} states, it can induce local Jahn-Teller distortion resulting in a low-spin state of Ni^{2+} ($S=0$).[25] Here some of the in-plane interaction can remain ferromagnetic but interplane Ni-O-Ni interaction can be both FM and AFM giving rise to a frustration in the lattice.

V. CONCLUSION

The important findings of the present study are summarized below:

(i) The cations are arranged both preferentially and randomly in the same structural unit giving rise to apparently two types of phases (ordered and random). The proportion of these two phases depends on composition and heat treatment.

(ii) The ac-χ shows a broad hump followed by a sharp peak at higher temperature for the samples with $x=0.3$ and 0.35. The hump at lower temperature is attributed to the random phase and the sharp peak seems to originate from the ordered phase in the samples.

(iii) The nature of field, frequency, and superimposed dc field dependence of this sharp peak in ac-χ as well as the field and history dependence of dc-χ allows us to conclude the presence of a spin-glass-like phase in the sample.

(iv) The evidence for a divergence in χ_3 makes the existence of a spin-glass-like phase more viable in this system.

(v) We have shown that our observations cannot be explained considering the presence of conventional ferrimagnetic, ferromagnetic, superparamagnetic, or cluster glass phases in the samples. It is even more difficult to reconcile our observations with other systems showing field and frequency dependence.

(vi) We have listed all possible exchange interactions in the system. We propose that the substitution introduces disorder in the planes and the intraplane along with the interplane interaction introduces frustration in the lattice.

ACKNOWLEDGMENTS

We would like to thank Professor R. Srinivasan, for many fruitful discussions and critical remarks. We acknowledge V. G. Sathe for helping in the Reitveld analysis and R. V. Krishnan for making dc magnetization measurements. A. Bajpai would like to acknowledge financial assistance from CSIR, India.

[1] J. B. Goodenough, D. G. Wickam, and W. J. Croft, J. Phys. Chem. Solids **5**, 107 (1958).
[2] W. Li, J. N. Reimers, and J. R. Dahn, Phys. Rev. B **46**, 3236 (1992).
[3] Jan N. Reimers, W. Li, and J. R. Dahn, Phys. Rev. B **47**, 8486 (1993).
[4] Jan N. Reimers, J. R. Dahn, J. E. Greedan, C. V. Stager, G. Liu, I. Davidson, and U. Von Sacken, J. Solid State Chem. **102**, 542 (1993).
[5] P. Ganguly, V. Ramaswamy, I. S. Mulla, R. F. Shinde, P. P. Bakare, S. Ganpathy, P. R. Rajmohanan, and N. V. K. Prakash, Phys. Rev. B **46**, 11 595 (1992).
[6] C. B. Azzoni, A. Paleari, V. Massarotti, M. Bini, and D. Capsoni, Phys. Rev. B **53**, 703 (1996).
[7] K. Hirakwa, H. Kadowaki, and K. Ubukoshi, J. Phys. Soc. Jpn. **55**, 323 (1985).
[8] J. P. Kemp, P. A. Cox, and J. W. Hodby, J. Phys. Condens. Matter **2**, 6699 (1990).
[9] P. Kuiper, G. Kruizinga, J. Ghijsen, and G. A. Sawatzky, Phys. Rev. Lett. **62**, 221 (1989).
[10] M. A. Van Veenendaal and G. A. Sawatzky, Phys. Rev. B **50**, 11 326 (1994).
[11] A. J. Bosman and C. Crevecoeur, Phys. Rev. **144**, 763 (1966).
[12] P. W. Anderson, Mater. Res. Bull. **8**, 153 (1973).
[13] K. Binder and A. P. Young, Rev. Mod. Phys. **58**, 803 (1986).
[14] Jean-Louis Tholence, in *Magnetic Susceptibility of Superconductors and other Spin Systems*, edited by Robert A. Hein, Thomas L. Francavilla, and Donald H. Liebenberg (Plenum, New York, 1991), p. 503.
[15] Masuo Suzuki, Prog. Theor. Phys. **58**, 1151 (1977).
[16] Suzumu Chikazawa, C. J. Sandberg, and Yoshihito Miyako, J. Phys. Soc. Jpn. **50**, 2884 (1981).
[17] T. Bitoh, K. Ohba, M. Takamatsu, T. Shirane, and S. Chikazawa, J. Magn. Magn. Mater. **154**, 59 (1996).
[18] R. A. Young, A. Sakthivel, T. S. Moss, and C. O. Paivasantos, *User's Guide to Program DBWS-9411* (Georgia Institute of Technology, Atlanta, 1994).
[19] S. Foner, Rev. Sci. Instrum. **30**, 548 (1959).
[20] Toshikaju Sato and Yoshihito Miyako, J. Phys. Soc. Jpn. **51**, 1394 (1981).
[21] A. Banerjee and A. K. Majumdar, Phys. Rev. B **46**, 8958 (1992).
[22] D. X. Chen and V. Skumryev, Phys. Rev. B **53**, 15 014 (1996).
[23] S. Van Houten, J. Phys. Chem. Solids **17**, 7 (1960).
[24] B. Goodenough, in *Magnetism and the Chemical Bond*, edited by F. A. Cotton (Wiley, New York, 1963).
[25] G. F. Dionne, J. Appl. Phys. **67**, 4561 (1990).